Electrorheological Fluids

Thomas C. Halsey

Suspensions of polarizable particles in nonpolarizable solvents form fibrillated structures in strong electric fields. The resulting increase in viscosity of these "electrorheological" fluids can couple electrical to hydraulic components in a servomechanism. The physical properties of these fluids are unusual owing to the long-range, anisotropic nature of the interparticle forces. Immediately after the electric field is applied, elongated chains or columns of particles form parallel to the field. This structure then coarsens as a result of thermal forces between the columns. In shear flows, fluids show yielding behavior at low stresses followed by shear-thinning behavior at higher stresses.

Electrorheological (ER) fluids are colloidal suspensions whose properties depend strongly and reversibly on the electric field. When fields are applied to these fluids, they respond by forming fibrous structures parallel to the applied field (Fig. 1). These fibers in turn greatly increase the viscosity of the fluid, by factors as high as 10^5. This interplay of electric fields, pattern formation, and viscosity is the key to both the engineering and the scientific importance of these fluids.

Electrorheological phenomena, sometimes referred to as the "Winslow effect," were first reported in detail by Willis Winslow in 1949 (*1*). He reported the following features of suspensions of silica gel particles in low-viscosity oils.

1) In an electric field of magnitude on the order of 3 kV/mm, the suspensions show a tendency to fibrillate, and highly elongated condensed structures of particles form parallel to the field.

2) A force proportional to the square of the electric field is necessary in order to shear the fluid between the electrical plates. Thus, at low shear stresses, the system behaves like a solid.

3) At stresses greater than this yield stress, the fluid flows like a viscous fluid, but with a large viscosity, again proportional to the square of the electric field.

These results of Winslow anticipated the three main themes of the study of the macroscopic properties of ER fluids: (i) structure formation in these fluids; (ii) yield stresses, or forces at which the behavior of the fluid changes from solid-like to liquid-like; and (iii) the viscous behavior of the fluid beyond the yield stress. Microscopic studies have concentrated on understanding the nature of the electrically induced forces between colloidal particles and on the synthesis of improved fluids for the purposes either of scientific studies or of applications. It is the development of greatly improved fluids that has reawakened interest in this field in the past decade.

The author is at the James Franck Institute and Department of Physics, University of Chicago, 5640 South Ellis Avenue, Chicago, IL 60637.

With ER fluids, it is possible to reversibly change the stress transmitted by a fluid over a large range. In order to take advantage of fast information processing in mechanical engineering, it is necessary to have a fast interface between an electric circuit and the mechanical response of a system. The ER response is extremely rapid; although full structure formation after the application of an electric field can take several seconds, the viscosity increases significantly over a time scale of 10^{-3} s. Practical devices that might be designed on the basis of this effect include variable-differential transmissions, shock absorbers, variable flow pumps, and other kinds of control devices (*2–4*).

A key design consideration is the amount of energy to be dissipated in the ER fluid itself. One of the most difficult tasks in the synthesis of ER fluids is the creation of fluids with properties that are stable over a large temperature range. Thus, applications such as clutches, in which a great deal of energy must be dissipated in the fluid, are intrinsically more challenging (and less likely to be attained soon) than control devices in which little energy is to be dissipated in the fluid. An intermediate case is the shock absorber. The response time of ER fluids is fast enough to make possible, at least in principle, active suspension systems in which the shock absorber characteristics are varied over short times to absorb the impact (of a New York City pothole, for example) in an optimal way (*5*). Fluids that can be used in shock absorbers will probably be synthesized within the next few years.

A crude model of the origin of the ER effect is shown in Fig. 2A. Suppose that the dielectric constant of the suspended particles is larger than that of the solvent. An electric field then polarizes the particles, leading to the appearance of induced charge at the particle surfaces. This charge creates a dipolar field around the particle, which can be modeled as a simple dipole moment $\mathbf{d} = \beta r_d^3 \mathbf{E}$, where β is an effective polarizability of the particle, r_d is its radius, and $\mathbf{E}$

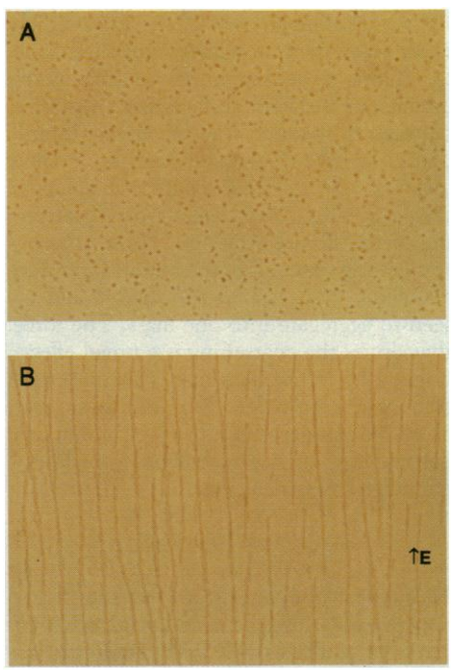

Fig. 1. (**A**) Isotropic suspension in the absence of an electric field. (**B**) Fibrillated structures in an electric field. Chains or columns of particles can be observed aligned with the electric field. The size of the particles is 0.7 μm. [Photos courtesy of J. E. Martin and J. Odinek, Sandia National Laboratories]

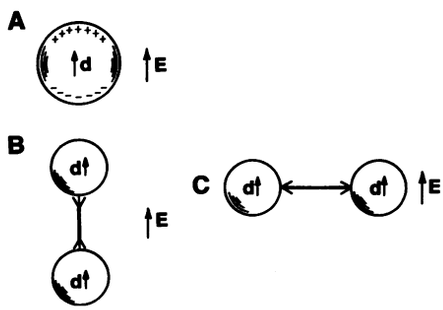

Fig. 2. (**A**) A particle whose dielectric constant is mismatched with the surrounding medium develops a dipole moment as a result of its polarization in an electric field. (**B**) Two such particles attract if they are arranged along the electric field direction or (**C**) repel if they are in the plane normal to the electric field direction.

is the electric field. The interaction energy u between two such polarizable particles is given by

$$u(r,\theta) = \frac{d^2}{r^3}(3\cos^2\theta - 1) \qquad (1)$$

where r is the distance between the particles and θ is the angle between the vector connecting the two particles and the electric field direction.

The force between two polarized particles, which can be obtained by differentiating Eq. 1, has two important features. In the first place, it is long-range, decaying as a power law r^{-4}, unlike the short-range interactions between particles more common in condensed matter or colloidal physics. In the second place, it is strongly anisotropic. Particles aligned along the field (Fig. 2B) attract one another, whereas particles in a plane perpendicular to the field (Fig. 2C) repel one another. There is a critical angle θ_c such that, if the angle θ satisfies $\theta < \theta_c \approx 55°$, then the interaction will be attractive; if $\theta > \theta_c$, the interaction will be repulsive. The force is proportional to the square of the dipole moment d^2; thus, it is proportional to E^2.

Several effects modify this situation in real fluids. For particles within a distance $\sim r_d$ of one another, where r_d is the particle radius, higher order multipolar interactions will be as important as the simple dipolar interaction (6). Furthermore, if the solvent is conducting at all, it will move charges to the particle surfaces in an attempt to screen the induced charge (7–9). This results in the same type of polarization as for dielectric spheres in a nonconducting fluid. The charges in the solvent around the particles lead to effective dipole moments for the particles, at least at long distances. Thus, theories formulated on the basis of dielectric constant mismatches have been qualitatively successful in describing the physics of the suspensions, even in the presence of finite conductivity solvents. If a high-frequency alternating electric field is applied, then there is not sufficient time in one cycle for charges to move from the solvent to the particle surfaces, and the dielectric polarization is indeed the source of the dipolar interactions.

The original slurries used by Winslow were too abrasive to be compatible with hydraulic pumping technology. In the early 1980s J. Stangroom and a group associated with Sheffield University in England developed a class of ER fluids made from ionic polymers with greatly improved properties (*10*). However, a further practical problem arises from absorbed water. Until recently, a large dielectric or conductivity mismatch was obtained between the particles and the solvent as a result of water absorbed in the particles. As regards applications, this is not a very attractive procedure: at high temperatures the water will tend to evaporate and the ER effect will be lost. More recently, anhydrous fluids (with no absorbed water) have been developed by the groups of Block at the Cranfield Institute of Technology (United Kingdom) and Filisko at the University of Michigan (*11*). These "third generation" ER fluids are very promising for future applications.

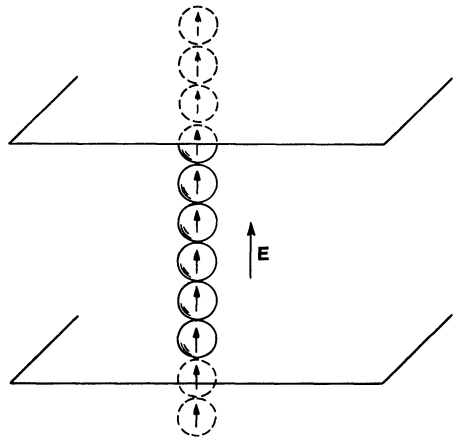

Fig. 3. Because the electrodes are at fixed potential, a chain of particles is accompanied by an image chain extending to infinity in both directions.

In this paper I will review structure formation, coarsening, and flow behavior of ER fluids. Structure formation takes place in two distinct phases. In the first, which takes place over an aggregation time scale t_a, chains or columns of particles form parallel to the field and span the distance between the walls of the cell. In the second phase, which is characterized by a time scale $t_c >> t_a$, these chains or columns slowly drift together, leading to a coarsening of the fibrous structure. After an arbitrarily long time, all of the chains (and thus all of the particles) in the fluid would be seen to aggregate into one mass. The force that drives the coarsening is a novel effect, originating in the Brownian (thermal) motion of the particles. In shear flows, the fibers no longer span the cell; one can determine their size by balancing hydrodynamic and electrical forces.

Structure Formation

Because of the anisotropy of the forces between individual particles, it is likely that chains of particles will form parallel to an applied electric field (Fig. 1). These chains are seen in experiment and typically span the entire distance between the electrodes. One can estimate the time for these chains to form by balancing the electrical forces against the viscous resistance of a solvent of viscosity μ_0. The typical aggregation time that is then obtained is $t_a \sim \mu_0/E^2$. This has been confirmed by Ginder and Elie, who observed this time scale for structure formation by multiple light scattering in a commercial ER fluid sample (*12*). They also observed a low-frequency (of the field) regime where aggregation time is inversely proportional to E, which seemed to arise from electrophoretic effects.

In addition to single chains, structures of several chains aggregated into roughly right-circular columns are also seen. It thus appears that the individual chains attract one another. This seems paradoxical: because the dipolar forces are repulsive for particles situated in a plane normal to the electric field, it might be expected that individual chains would repel one another.

However, this neglects the long-range nature of the force. A particle experiences the forces not only of a few particles in an adjacent chain but of the entire chain. Furthermore, just as an electric charge near a conducting surface has an image charge on the other side of the surface whose contribution should be included in computing the field, a chain of particles has an image chain that extends to infinity in both directions (Fig. 3) because of the presence of fixed-potential electrodes (*13*). The force between two such chains is very different from that between two particles. If the chains are displaced with respect to one another by a distance z in the direction parallel to the field and the distance between particle centers in the chain is $c \approx 2r_d$, then the force F between two chains of physical length L separated by a distance ρ is (*14, 15*)

$$F \propto L\cos(2\pi z/c)\exp(-\rho/c) \qquad (2)$$

This force is periodic in the direction along the chain, owing to the image forces. Thus, chains in register repel one another with a short-range force, whereas chains out of register attract one another. The force also decays exponentially with the transverse distance between the chains: a long-range interaction between particles leads to a short-range interaction between parallel chains. It is likely that the preferred state of a system of dipolar particles held between plates of fixed potential will thus be a solid of closely packed chains rather than a dispersed set of chains.

Electrorheological effects are not seen for arbitrarily small electric fields because of the Brownian motion of the colloidal particles, a ceaseless random motion caused by the temperature of the surrounding medium. Adriani and Gast have introduced a parameter λ that expresses the ratio of polarization to thermal forces (*16*)

$$\lambda = \frac{(\beta E)^2 r_d^3}{4\epsilon k_B T} \qquad (3)$$

where ϵ is the solvent dielectric constant, k_B is Boltzmann's constant, and T is the temperature.

Electrically determined structures are likely to occur only if the electrical forces can overcome the thermal forces. A dipolar solid will occur in the limit $\lambda >> 1$, in which thermal forces are small. In the opposite limit ($\lambda << 1$), no structure formation is likely, and the electric field may be treated as a small perturbation (*17*). For $\lambda \sim 1$, it is likely that a transition between these two regimes will occur; this criterion determines the threshold field (often on the order of less than a volt per millimeter) for ER effects.

Tao and Sun have studied the energies of various possible lattice structures in the limit $\lambda >> 1$ (*15, 18*). They concluded that the preferred lattice structure is a body-centered tetragonal structure consisting of an infinite number of chains packed together. This claim has been verified in the experiments of Chen *et al.*, who studied an ER suspension of glass spheres by using the transmitted patterns of a laser beam (*19*). They found good agreement between their results and the lattice structure proposed by Tao and Sun.

If the preferred state is a body-centered tetragonal lattice of unlimited extension in the direction perpendicular to the field, then one may ask why fibrillated structures are seen in the experiment. If the fibrillated structures are not the preferred state of the system, their origin should be explainable in terms of the physics of aggregation of the structures after an electric field has been applied.

A clue to this problem is provided by the work of Wilson and Taylor on the shape of dielectric liquid droplets in an electric field (*20*). The shape of these droplets is fixed by the competition between two physical effects: surface tension, which seeks to keep a liquid droplet spherical, and dielectric polarization effects, which seek to elongate a droplet in the direction of an applied electric field. This latter effect is the analog for a continuous system of the preference of two dipolar particles to align along the field rather than perpendicular to it.

For a condensed droplet of colloidal particles, a surface tension arises from the short-range ordering of the particles within the droplet (*13, 21*). However, this situation is different from that for an ordinary dielectric droplet: for ER fluids the energy scale that determines the surface tension varies as E^2, because the polarization forces are the dominant forces between the particles. Thus, the surface tension is intrinsically comparable to the volume polarization forces, and one cannot change the ratio of these forces by varying the electric field, as was done by Wilson and Taylor.

Because surface tension is a surface effect and polarization energies are a volume effect, volume effects will likely predominate as the size of a droplet increases. The balance between these two effects was studied by Halsey and Toor, who concluded that, if image forces can be disregarded, then the radius of a droplet in the direction parallel to the field ($r_\parallel$) is related to the radius in the direction perpendicular to the field ($r_\perp$) by (*13*)

$$r_\perp \sim r_\parallel^{2/3} r_d^{1/3} \quad (4)$$

When $r_\parallel \sim L$ (the distance between the electrodes), the droplet will begin to interact with its image droplets. It should then become elongated into a column of radius $R \sim L^{2/3} r_d^{1/3}$.

These arguments, which predict a characteristic width for the fibers, no longer apply in the high electric field limit $\lambda >> 1$. In this limit, the growth of the condensed domains is too fast to allow any equilibrium to be established between the surface energy and the polarization energy. There is a relaxation time t_r over which the surface tension is relevant; it can be shown that when $\lambda >> 1$, $t_a << t_r$, and the surface tension plays no role. For large values of λ, it is only possible to bound R by $R \leq L^{2/3} r_d^{1/3}$. In many experiments, the apparent diameter of the columns formed in the initial structure formation phase is close to that of one particle. In such cases, pure chains form, and the surface tension–driven regime discussed above is never attained. However, the thermodynamic ground state of the system is still a phase separation, which would correspond to all of the separated chains coming together to form one agglomeration. In the next section I will discuss the mechanism by which this takes place.

Coarsening

The coarsening of the structure after the initial columns or chains have formed is probably not driven solely by the electric field, owing to the short-range nature of the interaction (given by Eq. 2) for structures parallel to the field. These chain-like or columnar structures are never perfect, however. Colloidal particles exhibit Brownian motion, in which the random molecular collisions with a particle lead it to jerk around. Thus, the perfectly ordered columnar structures discussed above are always disturbed in some degree by this thermal motion of the dipolar particles.

One way of studying this problem is to consider the electric field near a thermally fluctuating column. The average electric field decays very quickly as one moves away from a column; however, owing to the fluctuations in the positions of the dipoles, a much larger fluctuating electric field appears away from the column (*14, 22*). At a transverse distance ρ from the column, the field will be primarily determined by fluctuations (transverse or longitudinal) of the column on a scale ρ. Although the field of such fluctuations decays as ρ^{-3}, the dipole moment associated with such a fluctuation is itself proportional to ρ. By equipartition, it is expected that the field energy density $E^2 \propto k_B T$. One then obtains

$$\sqrt{(E^2)} \sim \frac{\sqrt{k_B T R}}{\rho^2} \quad (5)$$

where the column radius R appears for dimensional reasons. A second column placed at a distance ρ from this column has a dipole moment per unit length proportional to $\beta R^2 E$. It will thus experience a typical force f per unit length whose order of magnitude will be

$$f \sim \frac{\sqrt{k_B T R} \beta E R^3}{\rho^3} \quad (6)$$

This force might be either repulsive or attractive, depending on the exact configuration of the fluctuating column. In either case, it will lead to motion of the other column. To compute this motion, it is necessary to include the effect of the restoring force for bending of the columns, which involves the energy scale $\beta^2 E^2 R^3$. This determines a characteristic length scale parallel to the field over which the motion of the columns will be coherent. In this way, one can estimate a time scale t_c during which columns of size R will collide with one another under the influence of these fluctuating forces. A value of $t_c \propto E^{-4/5}$ is obtained, which should be compared with $t_a \propto E^{-2}$. Thus, at large values of λ (large E), $t_c >> t_a$, and the time scale for the original column or chain formation is much shorter than the coarsening time (*23*). These theoretical arguments do not apply at low values of λ; nevertheless, thermal coarsening in the low-field regime, where $\lambda \sim 1$, has been observed in the molecular dynamics simulations of Toor (*24*).

This approach can also be used to compute the characteristic width of the columns as a function of time. One obtains

$$R(t) \propto t^{5/9} \quad (7)$$

This behavior should be contrasted with the ordinary growth of structure in a mixture of two phase-separating liquids (spinodal decomposition), for which $R(t) \propto t^{1/3}$ (*25*). The faster growth of structure for ER fluids is a consequence of the long-range forces in these fluids.

Qualitative observations of coarsening

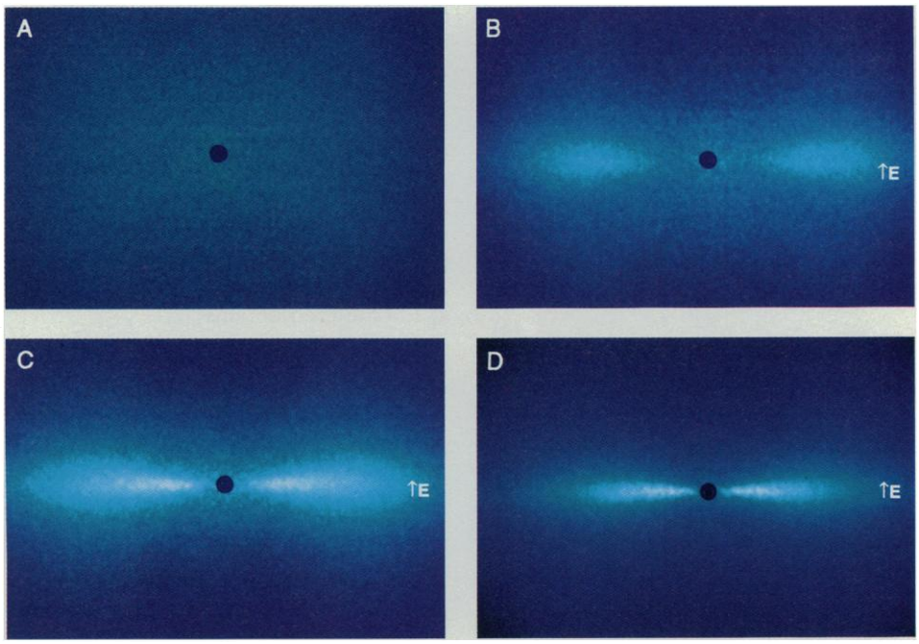

Fig. 4. Two-dimensional light scattering patterns of a coarsening ER fluid. The vertical direction corresponds to scattering with a wave-vector parallel to the field, the horizontal direction to scattering with a wave-vector perpendicular to the field. In (**A**) the pattern before the field is turned on is shown. This pattern is isotropic. (**B**), (**C**), and (**D**) show the development of structure after the field is turned on. The developing linear shape of the pattern reflects the orientation of the columns parallel to the electric field; the brighter areas correspond to the characteristic distance between these columns. These brighter areas move to positions of smaller wave-vector (larger distances) as time progresses. The circle at the center stops the unscattered laser beam. [Photos courtesy of J. E. Martin and J. Odinek, Sandia National Laboratories]

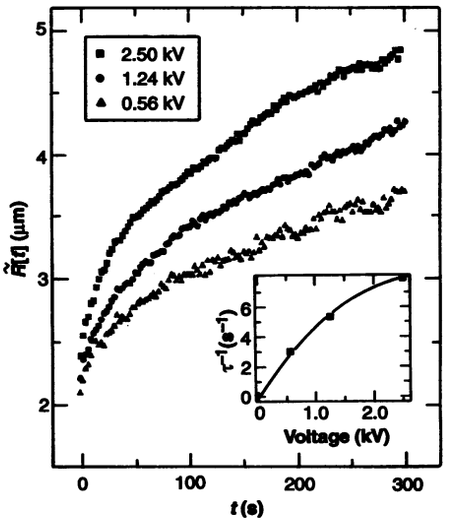

Fig. 5. The development of the length scale $\tilde{R}$ characterizing the structure in the direction transverse to the field ($\tilde{R} \propto R$, the typical column width). $\tilde{R}$ is determined by a scaling fit to scattering data and corresponds to the inverse wave vector of the strongest light scattering in, for example, Fig. 4. The best power law fit to this data is $\tilde{R} \propto t^{0.4}$, which is significantly faster than spinodal decomposition, owing to the long-range forces. The inset shows the dependence of growth rate on electric field, which agrees with the theory discussed in the text. [Data courtesy of J. E. Martin and J. Odinek, Sandia National Laboratories]

have been reported by numerous groups. In the experiment of Chen *et al.* (*19*), coarsening over time scales of several minutes resulted in the formation of 0.6-mm-diameter columns comprised of 20- to 40-μm particles.

This phenomenon has also been studied experimentally by Martin *et al.* at Sandia National Laboratories (*22*). They used index-matched ER fluids for which light scattering could be used to probe the development of structure for times up to hundreds of seconds. After the field was turned on, they found a scattering pattern from a three-dimensional sample that resembled a *p*-lobe structure, which then collapsed down into the plane normal to the electric field (Fig. 4). This behavior corresponds to a very rapid formation of one-dimensional columnar structures over time scales of less than a second. Over time scales of tens to hundreds of seconds, they observed the coarsening of this structure; the length scale $R(t)$ corresponding to the maximum in-plane scattering obeyed $R(t) \propto t^{0.4\pm0.1}$ (Fig. 5), which is in semiquantitative agreement with the model described above and with Eq. 7 in particular. The scattering peaks that corresponded to the columnar ordering were not Bragg peaks, but were broad peaks more characteristic of spinodal decomposition in their shape, although not in their time development.

Yield Stresses and Rheology

Understanding the structure of ER fluids allows one to examine the rheological properties that give ER fluids their practical importance. In the standard experimental geometry for flow studies, there are two parallel electrodes. One electrode plate is fixed, whereas the other slides parallel to itself to produce a shear flow. As one electrode is sheared with respect to the other, a finite force (yield stress) may be necessary before the plate will move freely. Beyond this threshold, the restoring force will be determined by the apparent macroscopic viscosity of the suspension. If this viscosity decreases as the shear rate is increased, then the fluid is said to be "shear-thinning."

Many experiments on ER suspensions have observed a yield stress (*1*, *26*, *27*). Klingenberg and Zukoski have proposed a simple argument in which they suggest that a finite shear force is necessary to destroy the columnar or chain-like structures (*28*). Considering a chain inclined at an angle θ to the electric field, one sees that beyond the angle $\theta_c \approx 55°$ the dipolar forces become repulsive, and the structure will disintegrate. Because the restoring force on the stretched chain is $\sim\beta^2E^2r_d^2$, one expects a yield stress τ_0

$$\tau_0 \sim \phi\beta^2E^2 \qquad (8)$$

where ϕ is the volume fraction of the particles. This model assumes that the particles are effectively pinned at the electrodes so that chains break at some distance from the electrodes before they detach from the electrodes.

The quantitative value of this yield stress has been the subject of considerable confusion. The value calculated from a simple dipolar force is significantly smaller than the values obtained from experiment, suggesting that other, short-range interactions are responsible for much of the yield stress. Klingenberg computed multipolar contributions to the yield stress and found values more in agreement with the experimental results (*29*).

Numerous groups have been shear-thinning behavior beyond this threshold. The natural parameter to describe the hydrodynamic behavior of ER fluids is the Mason number (*Mn*), which describes the ratio of viscous to electrical forces, and is given by (*30*)

$$Mn = \frac{24\pi\epsilon\mu_0\dot{\gamma}}{(\beta E)^2} \qquad (9)$$

where $\dot{\gamma}$ is the (dimensionless) strain rate, μ_0 is the solvent viscosity, β is the effective

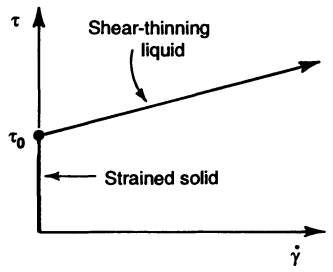

Fig. 6. Stress τ versus strain rate $\dot{\gamma}$ for a Bingham plastic. A finite yield stress τ_0 is necessary to induce flow; beyond this threshold, the excess stress $\tau - \tau_0$ is proportional to $\dot{\gamma}$.

polarizability of the particles, and ϵ is the solvent dielectric constant.

Marshall *et al.* observed a viscous response that seemed to depend only on this combination of strain rate and electric field (*30*). Further experiments of Klingenberg and Zukoski also demonstrated the development of boundary layers in shear flows (*28*). These boundary layers consisted of the regions of essentially condensed particles near the electrodes; in these regions, the solvent flowed with the electrode. The flow gradient was concentrated in a gap halfway between the two electrodes. By equating the hydrodynamic stress at the edge of this gap with the yield stress of the full ER structures, Klingenberg and Zukoski predicted a "Bingham plastic" type of behavior, shown in Fig. 6, with the stress τ given as a function of strain rate $\dot{\gamma}$ by

$$\tau = \tau_0 + \mu_\infty \dot{\gamma} = \tau_0(1 + aMn) \quad (10)$$

where μ_∞ is the viscosity of the fluid at large strain rates and a is a numerical constant ~ 1. The differential viscosity $d\tau/d\dot{\gamma}$ does not vary with electric field; it is rather the apparent suspension viscosity, $\mu_s = \tau/\dot{\gamma} \propto Mn^{-1}$, that varies with the field (this is the quantity that I have called the "viscosity" until now). The Bingham model accounted reasonably well for the observations of Klingenberg and Zukoski and of Marshall *et al.*

An alternative model was proposed by Halsey, Martin, and Adolf (*31*). Consider a condensed droplet of dipolar particles. A shear flow will tend to rotate such a region; on the other hand, the electric field will exert a restoring torque that will attempt to restore such a "droplet" to a position parallel to the field (Fig. 7). By balancing the hydrodynamic torque arising from the shear flow against this electrical torque, one obtains a characteristic angle between the long axis of the droplet and the electric field for a droplet of any size.

This characteristic angle increases as the size of the droplet increases because it becomes more and more difficult for the droplet to remain vertical with respect to the field as it extends further and further into the shear flow. If a droplet is oriented at too large an angle with respect to the field, it is no longer advantageous for such a droplet to form because its polarization energy is not sufficiently large.

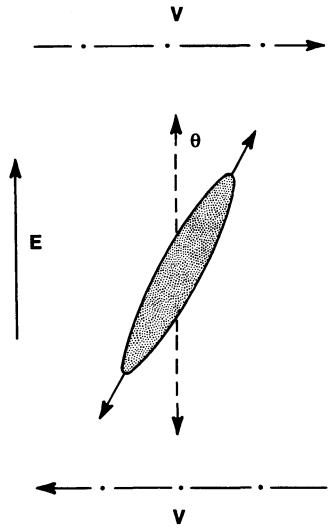

Fig. 7. A dielectric droplet will be rotated by a shear flow. Its equilibrium angle θ will be determined by a balance between the electrical and the hydrodynamic torques.

There is thus a characteristic size of droplet that minimizes the polarization energy. Droplets in a shear flow are constantly sheared with respect to one another; in the process the droplets collide and agglomerate, as well as break up, constantly. It is thus tempting to regard the distribution of droplets as sufficiently ergodic that the characteristic droplet size is precisely one that minimizes the polarization energy. Alternatively, one can observe that the collision of two droplets, both much smaller than this size, will tend to stably lead to the formation of larger droplets, whereas droplets above this characteristic size will be unstable toward breakup into smaller droplets. Thus, it is natural to expect that this energetically favorable size will characterize the droplet distribution. Direct optical observation of droplets in low-concentration shear flows confirms this suspicion. "Droplets" of a few particles have also been observed in molecular dynamics simulations of shear flow by Bonnecaze and Brady (*32*).

In the droplet model, the Mason number determines the typical angle of the droplets with respect to the field, as well as the characteristic droplet size. The angle θ with respect to the field is given by

$$\theta \sim Mn^{1/3} \quad (11)$$

and the length l of the droplet is given by

$$\frac{l}{r_d} \sim Mn^{-1} \quad (12)$$

It is then easy to estimate the viscosity of the suspension μ_s as a function of Mn and the solvent viscosity μ_0.

$$\mu_s \sim \phi\mu_0 Mn^{-2/3} \quad (13)$$

These predictions are in partial agreement with the experimental results of Halsey, Martin, and Adolf, which were obtained from the same index-matched fluids referred to in the discussion of coarsening above (*31*). They indeed found that μ_s scaled with a power law in $\dot{\gamma}$ as $\mu_s \propto \dot{\gamma}^{-\Delta}$. At relatively low electric field strengths, they found $\Delta \approx 0.68$, in agreement with the value predicted by the droplet model. However, at higher electric field strengths they found somewhat larger values of Δ; at the highest field strength they found $\Delta \approx 0.9$, which is close to the Bingham behavior proposed by Klingenberg and Zukoski (*28*). This suggests that boundary layers may have played a role in this experiment. A troubling aspect of this experiment is that the experimenters could not fully describe the dependence of the viscosity on electric field by the Mason number alone, implying either that thermal effects were relevant in these experiments (despite their large values of λ) or that the energy scale of electrical interactions between the particles was not proportional to E^2, perhaps as a result of charging effects in the solvent around the particles.

In these experiments, no yield stress was observed; the fluid exhibited observable flow at the lowest stresses, although this flow declined to zero as a power law in stress

$$\tau \propto \dot{\gamma}^{1-\Delta} \quad (14)$$

One possible explanation for the discrepancy between this result and that of Klingenberg and Zukoski and others is that the yield stress may depend on the ability of particles to bind to the surface. This would imply in turn that surface preparation may be significant in determining the rheological properties of the suspensions.

Conclusions

In this review I have outlined a picture in which structures form over a time scale t_a and coarsen by means of a thermal mechanism over a time scale t_c. In shear flows, an equilibrium is established between hydrodynamic and electrical forces which determines the scale of the structures that appear. These ideas only begin to outline the science of ER fluids.

Some ER phenomena are reminiscent of ferrofluids, which are better understood. Ferrofluids are suspensions of permanently magnetized particles of size ~ 10 nm (*33*). However, in order to prevent permanent aggregation, ferrofluid particles have magnetic interaction energies at contact that are always less than or on the order of k_BT.

Thus, ER phenomena resulting from the ability to attain large values of λ will have no analogs in ferrofluids. Furthermore, the image forces that play a large role in the macroscopic behavior of ER fluids do not exist for ferrofluids, which are generally studied in solenoidal fields. One can impose pseudosolenoidal fields on ER fluids by operating at high frequencies and inserting a nonconducting dielectric between the electrodes and the fluid; however, no significant experiments have been conducted in this geometry.

From both an engineering and a scientific point of view, a better understanding of the microscopic mechanisms of interaction between particles and between particles and electrode surfaces is needed. Such an understanding would be very helpful in synthesizing fluids with superior properties. I have hardly touched on this subject in this review; many topics, such as the role of polydispersity, or the nature of solid structures beyond the idealized Tao and Sun model, have not been addressed here.

I have also not discussed the nature of the early phases of aggregation. Aside from the time scale and some preliminary analyses of the scaling (*34*), very little work has been done on the early phases of aggregation, which is perhaps the area that can most easily be studied by the techniques of molecular dynamics. More detailed theories of late-stage aggregation and rheological response, which go beyond the rather simple arguments above, are also needed.

REFERENCES AND NOTES

1. W. Winslow, *J. Appl. Phys.* **20**, 1137 (1949).
2. Z. P. Shulman, R. G. Gorodkin, E. V. Korobko, V. K. Gleb, *J. Non-Newtonian Fluid Mech.* **8**, 29 (1981).
3. D. Scott and J. Yamaguchi, *Autom. Eng.* **93**, 75 (1985).
4. T. G. Duclos, D. N. Acker, J. D. Carlson, *Mach. Des.* (21 January 1988), p. 42.
5. D. L. Hartsock, R. F. Novak, G. J. Chaundy, *J. Rheol.* **35**, 1305 (1991).
6. H. A. Pohl, *Dielectrophoresis* (Cambridge Univ. Press, Cambridge, 1978).
7. D. L. Klass and T. W. Martinek, *J. Appl. Phys.* **38**, 67 (1967).
8. Y. F. Deinega and G. V. Vinogradov, *Rheol. Acta* **23**, 636 (1984).
9. L. C. Davis, *Appl. Phys. Lett.* **60**, 319 (1992).
10. J. E. Stangroom, *Phys. Technol.* **14**, 290 (1983).
11. H. Block and J. P. Kelly, *J. Phys. D* **21**, 1661 (1985); U.S. Patent No. 4,687,589 (1987); F. E. Filisko and W. H. Armstrong, U.S. Patent No. 4,744,914 (1988); F. E. Filisko and L. H. Radzilowski, *J. Rheol.* **34**, 539 (1990).
12. J. M. Ginder and L. D. Elie, in *Proceedings of the Conference on Electrorheological Fluids*, Carbondale, IL, R. Tao, Ed. (World Scientific, Singapore, 1992), pp. 23–36.
13. T. C. Halsey and W. R. Toor, *Phys. Rev. Lett.* **65**, 2820 (1990).
14. ———, *J. Stat. Phys.* **61**, 1257 (1990).
15. R. Tao and J. M. Sun, *Phys. Rev. Lett.* **67**, 398 (1991).
16. P. M. Adriani and A. P. Gast, *Phys. Fluids* **31**, 2757 (1988); all relevant dimensionless groups are reviewed in A. P. Gast and C. F. Zukoski, *Adv. Colloid Interface Sci.* **30**, 153 (1989).
17. P. G. De Gennes and P. Pincus, *Phys. Kondens. Mater.* **11**, 189 (1970); P. C. Jordon, *Mol. Phys.* **25**, 961 (1973).
18. R. Tao and J. M. Sun, *Phys. Rev. A* **44**, 6181 (1991).
19. T.-J. Chen, R. N. Zitter, R. Tao, *Phys. Rev. Lett.* **68**, 2555 (1992).
20. C. T. R. Wilson and G. I. Taylor, *Proc. Cambridge Philos. Soc.* **22**, 728 (1925); for a recent application, see J. C. Bacri and D. Salin, *J. Phys. (Paris) Lett.* **43**, 1 (1982).
21. W. R. Toor and T. C. Halsey, *Phys. Rev. A* **45**, 8617 (1992).
22. J. E. Martin, J. Odinek, T. C. Halsey, *Phys. Rev. Lett.* **69**, 1524 (1992).
23. For other examples of thermally generated interactions, see W. Helfrich, *Z. Naturforsch. Teil A* **33**, 305 (1978); S. N. Coppersmith, D. S. Fisher, B. I. Halperin, P. A. Lee, W. F. Brinkman, *Phys. Rev. Lett.* **46**, 549 (1981); D. R. Nelson, *J. Stat. Phys.* **57**, 511 (1989).
24. W. Toor, *J. Colloid Interface Sci.*, in press.
25. E. M. Lifshitz and L. P. Pitaevski, *Physical Kinetics* (Pergamon Press, Oxford, ed. 2, 1981), chap. 12.
26. H. Uejima, *Jpn. J. Appl. Phys* **11**, 319 (1972).
27. C. M. Cerda, R. T. Foister, S. G. Mason, *J. Colloid Interface Sci.* **82**, 577 (1981).
28. D. J. Klingenberg and C. F. Zukoski, *Langmuir* **6**, 15 (1990).
29. D. J. Klingenberg, thesis, University of Illinois, Urbana-Champaign (1988).
30. L. Marshall, C. F. Zukoski, J. Goodwin, *J. Chem. Soc. Faraday Trans. I* **85**, 2785 (1989).
31. T. C. Halsey, J. E. Martin, D. Adolf, *Phys. Rev. Lett.* **68**, 1519 (1992); a similar model was proposed for "magneto-rheological" fluids by Z. P. Shulman *et al.*, *Int. J. Multiphase Flow* **12**, 935 (1986).
32. R. T. Bonnecaze and J. F. Brady, *J. Chem. Phys.* **96**, 2183 (1992). Another study that explores the large Mason number regime is in J. Melrose, *Phys. Rev. A* **44**, 4789 (1991).
33. An excellent general discussion of ferrofluids can be found in R. E. Rosensweig, *Ferrohydrodynamics* (Cambridge Univ. Press, New York, 1985).
34. H. See and M. Doi, *J. Phys. Soc. Jpn.* **60**, 2778 (1991).

35. I am grateful to J. E. Martin, S. Nagel, and T. A. Witten for critical readings of the manuscript. D. Adolf, J. E. Martin, J. Odinek, and W. Toor collaborated on various aspects of this work, which was partially funded by the National Science Foundation through a Presidential Young Investigator award, DMR-9057156. Acknowledgement is made to the donors of the Petroleum Research Fund for the partial support of this research.

What If Minkowski Had Been Ageusic? An Alternative Angle on Diabetes

J. Denis McGarry

Despite decades of intensive investigation, the basic pathophysiological mechanisms responsible for the metabolic derangements associated with diabetes mellitus have remained elusive. Explored here is the possibility that traditional concepts in this area might have carried the wrong emphasis. It is suggested that the phenomena of insulin resistance and hyperglycemia might be more readily understood if viewed in the context of underlying abnormalities of lipid metabolism.

Recognized since the time of Aristotle, diabetes mellitus is now known to encompass a variety of syndromes with distinct etiologies that collectively afflict 1 to 6% of the population in the United States. Of these, 10 to 25% fall into the category of insulin-dependent diabetes mellitus (IDDM), which generally appears before age 40, frequently in adolescence, and results from autoimmune destruction of insulin-producing cells within the pancreas. Far more common is non–insulin-dependent diabetes mellitus (NIDDM) which, at least in its early stages, is characterized not by insulin deficiency but by the failure of the hormone to act efficiently in target tissues such as muscle, liver, and fat. Unlike IDDM, NIDDM is often associated with obesity (*1*). In this article, I will examine fuel metabolism in diabetes, with a view to advancing a key role for the lipid component.

Regardless of type, uncontrolled diabetes represents a serious disruption of fuel homeostasis with ravaging consequences throughout the body. Although much has been learned, current knowledge remains largely descriptive, consisting mainly of an ever expanding list of the metabolic, vascular, and neurological abnormalities that accompany the active disease process. What has not yet emerged, despite immense investment of resources, is a clear understanding of the basic pathophysiological mechanisms of diabetes and their temporal relations to each other.

Why has this problem remained so intractable? A major contributing factor has been that, compared with other hormones, insulin elicits a bewildering array of metabolic responses in target cells. Deciding

The author is in the Departments of Internal Medicine and Biochemistry and the Center for Diabetes Research, University of Texas Southwestern Medical Center at Dallas, 5323 Harry Hines Boulevard, Dallas, TX 75235.